Polyhedron 154 (2018) 325–333

Contents lists available at ScienceDirect

Polyhedron

journal homepage: www.elsevier.com/locate/poly

Synthesis, structural characterization and antimicrobial activity of silver (I) complexes with 1-benzyl-1*H*-tetrazoles

Tina P. Andrejević [a,1], Andrea M. Nikolić [b,1], Biljana Đ. Glišić [a,*], Hubert Wadepohl [c], Sandra Vojnovic [d], Mario Zlatović [b], Miloš Petković [e], Jasmina Nikodinovic-Runic [d], Igor M. Opsenica [b,*], Miloš I. Djuran [f]

[a] University of Kragujevac, Faculty of Science, Department of Chemistry, R. Domanovića 12, 34000 Kragujevac, Serbia
[b] University of Belgrade-Faculty of Chemistry, Studentski trg 16, 11158 Belgrade, Serbia
[c] Anorganisch-Chemisches Institut, University of Heidelberg, Im Neuenheimer Feld 270, 69120 Heidelberg, Germany
[d] Institute of Molecular Genetics and Genetic Engineering, University of Belgrade, Vojvode Stepe 444a, 11000 Belgrade, Serbia
[e] Department of Organic Chemistry, Faculty of Pharmacy, University of Belgrade, 11000 Belgrade, Serbia
[f] Serbian Academy of Sciences and Arts, Knez Mihailova 35, 11000 Belgrade, Serbia

ARTICLE INFO

Article history:
Received 26 June 2018
Accepted 2 August 2018
Available online 11 August 2018

Keywords:
1-Benzyl-1*H*-tetrazoles
Silver(I) complexes
Structural characterization
Antimicrobial activity
Cytotoxicity

ABSTRACT

Herein, we report the synthesis and structural characteristics of three tetrazole-containing compounds, 1-benzyl-1*H*-tetrazole (bntz), 1-benzyl-1*H*-tetrazol-5-amine (bntza) and 1-(4-methoxybenzyl)-1*H*-tetrazol-5-amine (mbntza) and the corresponding silver(I) complexes of the general formula $[Ag(NO_3\text{-}O)(L\text{-}N4)_2]_n$, L = bntz (**1**), bntza (**2**) and mbntza (**3**). Silver(I) complexes **1**–**3** and 1-benzyl-1*H*-tetrazoles have been studied in detail by NMR, IR and UV–Vis spectroscopic methods and the structures of **1** and **2** have been determined by single-crystal X-ray diffraction analysis. The results of these analyses revealed a monodentate coordination of the ligands to Ag(I) ion *via* the N4 tetrazole nitrogen. The antimicrobial potential of silver(I) complexes **1**–**3** was evaluated against the broad panel of Gram-positive and Gram-negative bacteria and fungi, displaying their remarkable inhibiting activity with MIC (minimal inhibitory concentration) values in the range 2–8 and 0.16–1.25 μg/mL (3.8–16.3 and 0.31–2.15 μM), respectively. On the other hand, 1-benzyl-1*H*-tetrazoles used for the synthesis of the silver(I) complexes were not active against the investigated strains, suggesting that the activity of the complexes originates from the Ag(I) ion exclusively. Moreover, silver(I) complexes **1**–**3** have good therapeutic potential, which can be deduced from their moderate cytotoxicity on the human fibroblast cell line MRC5, with IC_{50} values falling in the range 30–60 μg/mL (57.7–103.4 μM).

1. Introduction

Silver(I) complexes exhibit a wide range of applications in the medicinal and analytical chemistry, catalysis and the polymer design [1,2]. The use of silver(I) complexes in medicine is mainly related to their well known antibacterial and antifungal properties which are attributed to the presence of Ag(I) ion [3–6]. This metal ion is highly toxic to microorganisms, well tolerated by mammalians and does not present a serious toxic risk to human body [7,8]. Nevertheless, silver poisoning can occur among people chronically exposed to this metal [5]. Thus, argyria, the permanent discoloration of the skin, has been observed in persons that have ingested both metallic silver and silver(I) compounds in small doses during a long time period [5]. Although most scientists believe that argyria is the most serious health effect caused by the silver, there are also a few reports claiming that silver can cause brain damage, seizure or a persistent vegetative state [5].

In comparison to the simple silver(I) salts, the complexes of this metal ion represent an alternative formulation of silver with tunable antimicrobial properties. Many silver(I) complexes have shown superior antimicrobial activity in comparison with the silver(I) salts [1,9], as well as lower *in vitro* cytotoxicity on the healthy human lung fibroblast cell line MRC5 and *in vivo* embryotoxicity [10]. One of the key factors determining the antimicrobial potential of silver(I) complexes is the type of donor atom coordinated to Ag(I) ion and, consequently, the rate of the ligand replacement rather than the complexes' solubility, charge and degree of polymerization [11]. For instance, silver(I) complexes with nitrogen donors have shown an effective and wide-spectrum antimicrobial activity [11–13]. The effectiveness of this type of silver(I)

* Corresponding authors. Fax: +381 34 335 040 (B.Đ. Glišić).
E-mail addresses: bglisic@kg.ac.rs (B.Đ. Glišić), igorop@chem.bg.ac.rs (I.M. Opsenica).
[1] T.P.A. and A.M.N. contributed equally.

https://doi.org/10.1016/j.poly.2018.08.001
0277-5387/

complexes was connected with the presence of a weak Ag—N bond, which can be easily cleaved in their interaction with different biomolecules, such as thiol-containing proteins and nucleic acids, the process that is supposed to be a prerequisite for their antimicrobial action [6,11–13].

Aromatic nitrogen-containing heterocyclic compounds (*N*-heterocycles) are one of the most important class of the nitrogen donor ligands utilized in the synthesis of biologically active silver(I) complexes [6]. These compounds represent structural moieties of many natural products and biologically important molecules, as well as pharmacologically used agents [14]. So far, different *N*-heterocycles such as imidazole and its substituted derivatives [7,15–18], tetrazole [19], pyridine and its derivatives [20–24], quinolines [25], diazines and benzodiazines [9,10,26], bipyridines [27], terpyridines [28] and phenantrolines [29–36] have been used for the synthesis of mono- and polynuclear silver(I) complexes, which have shown a remarkable activity against a broad panel of bacterial and fungal strains which can lead to many infections.

Even though tetrazoles, five-membered aromatic heterocycles which contain four nitrogen atoms within one ring, are not a part of any natural product, they have attracted considerable attention as structural components of energetic materials [37], bioactive compounds [38], nanomaterials [39] and as ligands for complexation to different metal ions [40–42]. Besides the unsubstituted tetrazole, there is a growing interest in the investigation of compounds containing *N*-linked substituents attached to the ring carbon of tetrazole, especially for 5-amino-1*H*-tetrazole and its derivatives [40]. 5-Amino-1*H*-tetrazole motif is interesting, because it is nitrogen-rich compound which possesses five potential binding sites (one amino and four tetrazole nitrogen atoms) [43].

Herein, we have synthesized 1-benzyl-1*H*-tetrazole (bntz), 1-benzyl-1*H*-tetrazol-5-amine (bntza) and 1-(4-methoxybenzyl)-1*H*-tetrazol-5-amine (mbntza), all containing 1-benzyl-1*H*-tetrazole motif [44] and used them as ligands for the synthesis of silver(I) complexes of the general formula $[Ag(NO_3\text{-}O)(L\text{-}N4)_2]_n$, L = bntz (**1**), bntza (**2**) and mbntza (**3**) (Scheme 1). The 1-benzyl-1*H*-tetrazoles and the corresponding silver(I) complexes were evaluated for *in vitro* antimicrobial and antiproliferative activities against the normal human lung fibroblast cell line to properly address their therapeutic potential.

2. Experimental

2.1. Materials and methods

Unless stated otherwise, all solvents and reagents were obtained from commercial sources and used without further purification. Elemental microanalyses of the synthesized 1-benzyl-1*H*-tetrazoles and silver(I) complexes for carbon, hydrogen and nitrogen were performed by the Microanalytical Laboratory, Faculty of Chemistry, University of Belgrade. The IR spectra were recorded as KBr pellets on a Perkin Elmer Spectrum 100 spectrometer over the wavenumber range of 4000–450 cm^{-1}. The NMR spectra of the 1-benzyl-1*H*-tetrazoles and silver(I) complexes were recorded at 25 °C on a Bruker Avance III Ultrashield (^1H at 500 MHz, ^{13}C at 125 MHz) and Bruker Avance III 400 MHz

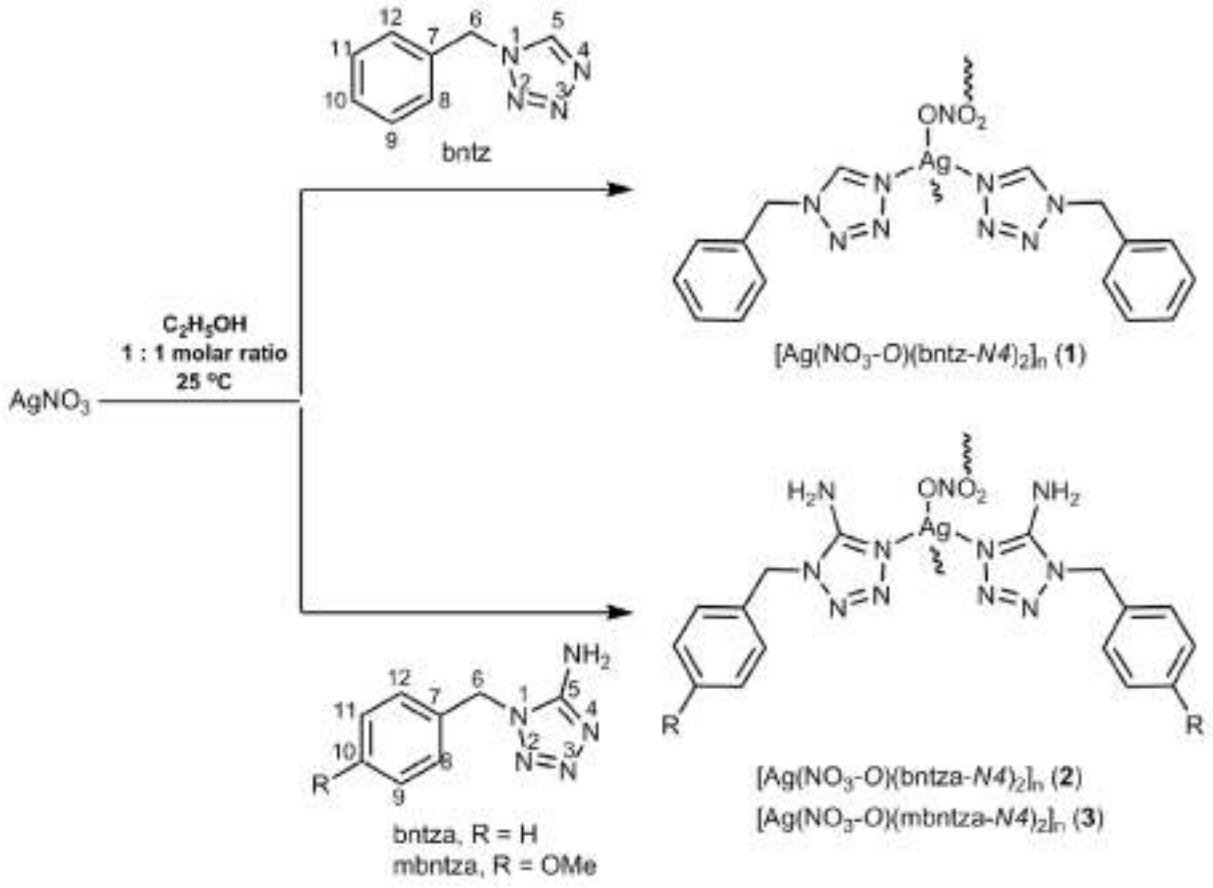

Scheme 1. Schematic presentation of the reactions for the synthesis of the silver(I) complexes **1**–**3**. Numbering scheme of nitrogen and carbon atoms in 1-benzyl-1*H*-tetrazoles does not match the one applied in the X-ray study of silver(I) complexes **1** and **2**.

spectrometer (^{1}H at 400 MHz, ^{13}C at 101 MHz), respectively. In order to investigate the solution stability of silver(I) complexes, the ^{1}H NMR spectra were recorded immediately after their dissolution in DMSO-d_6, as well as after 48 h standing in the dark at room temperature. The UV–Vis spectra were recorded on a Shimadzu spectrophotometer in DMSO/H_2O (1:9, v/v). Compounds bntza and mbntza were analyzed by high resolution tandem mass spectrometry using LTQ Orbitrap XL (Thermo Fisher Scientific Inc., USA) mass spectrometer. The sample was dissolved in CH_3CN and it was injected directly. Ionization was done in positive mode on heated electrospray ionization (HESI) probe. HESI parameters were: spray voltage 4.7 kV, vaporizer temperature 60 °C, sheath and auxiliary gas flow 24 and 10 (arbitrary units), respectively, capillary voltage 49 V, capillary temperature 275 °C, tube lens voltage 80 V, resolution (at *m/z* 400): 30000.

2.2. Synthesis of 1-benzyl-1H-tetrazoles

The tetrazole-containing compounds, 1-benzyl-1*H*-tetrazole (bntz), 1-benzyl-1*H*-tetrazol-5-amine (bntza) and 1-(4-methoxybenzyl)-1*H*-tetrazol-5-amine (mbntza), were synthesized by previously described methods [45,46]. These compounds were pure based on elemental microanalysis and NMR spectroscopy.

2.2.1. 1-Benzyl-1H-tetrazole (bntz)

1-Benzyl-1*H*-tetrazole (bntz) was synthesized according to the procedure described by Satoh and Marcopulos as a yellow crystalline solid (see Supplementary data) [45]. Yield: 40% (598.0 mg). Mp 52–55 °C. IR (KBr, *ν*, cm^{-1}): 3113, 3065 (*ν*(C_{ar}—H)), ~3000 (*ν*(C—H)), 1670 (*ν*(C_{ar}=N)), 1495 (*ν*(N—C_{ar}=N)), 1465 (*δ*(CH_2)), 1386 (*ν*(N=N)), 1243 (*ν*(C—N)), 1162 (*ν*(N—N)), 710 (*γ*(Car—H)). ^{1}H NMR (500 Hz, $CDCl_3$): *δ* 5.60 (*s*, 2H, C6H), 7.29–7.32 (*m*, 2H, C8H and C12H), 7.38–7.42 (*m*, 3H, C9H–C11H), 8.57 ppm (*s*, 1H, C5H). ^{13}C{^{1}H} NMR (125 Hz, $CDCl_3$): *δ* 52.09 (C6), 128.23 (C8 and C12), 129.29 (C10), 129.33 (C9 and C11), 132.78 (C7), 142.38 ppm (C5). UV–Vis (DMSO/H_2O, λ_{max}, nm): 257.0 ($\varepsilon = 3.6{\cdot}10^2$ M^{-1} cm^{-1}).

2.2.2. 1-Benzyl-1H-tetrazol-5-amine (bntza)

The amino-containing bntza compound was synthesized according to the previously reported method as a colorless solid (see Supplementary data) [46]. Yield: 59% (939.0 mg). Mp 184–186 °C. IR (KBr, *ν*, cm^{-1}): 3338 (ν_{as}(NH_2)), 3153 (ν_s(NH_2)), 3064 (*ν*(C_{ar}—H)), ~3000 (*ν*(C—H)), 1642 (*ν*(C_{ar}=N)), 1485 (*ν*(N—C_{ar}=N)), 1430 (*δ*(CH_2)), 1336 (*ν*(N=N)), 1269 (*ν*(C—N)), 1125 (*ν*(N—N)), 723 (*γ*(Car—H)). ^{1}H NMR (500 Hz, DMSO-d_6): *δ* 5.35 (*s*, 2H, C6H), 6.82 (*s*, 2H, NH_2), 7.20–7.24 (*m*, 2H, C8H and C12H), 7.28–7.32 (*m*, 1H, C10H), 7.33–7.38 ppm (*m*, 2H, C9H and C11H). ^{13}C{^{1}H} NMR (125 Hz, DMSO-d_6): *δ* 47.53 (C6), 127.52 (C8 and C12), 127.93 (C10), 128.70 (C9 and C11), 135.41 (C7), 155.52 ppm (C5). UV–Vis (DMSO/H_2O, λ_{max}, nm): 238.0 ($\varepsilon = 2.4{\cdot}10^3$ M^{-1} cm^{-1}). HRMS (HESI/Orbitrap) *m/z* [M+H]$^+$ calc for $C_8H_{10}N_5$: 176.09362; found 176.09299.

2.2.3. 1-(4-Methoxybenzyl)-1H-tetrazol-5-amine (mbntza)

Following the procedure described for bntza [46], compound mbntza was obtained from 4-(methoxyphenyl)methanamine as a colorless crystalline solid. Yield: 62% (185.0 mg). Mp 183–185 °C. IR (KBr, *ν*, cm^{-1}): 3332 (ν_{as}(NH_2)), 3162 (ν_s(NH_2)), 3025, 2961 (*ν*(C_{ar}—H)), 2840, 2742 (*ν*(C—H)), 1660 (*ν*(C_{ar}=N)), 1513 (*ν*(N—C_{ar}=N)), 1458 (*δ*(CH_3)), 1436 (*δ*(CH_2)), 1307 (*ν*(N=N)), 1281 (*ν*(C—N)), 1253 (*ν*(C—O)), 1182 (*ν*(N—N)), 792, 677 (*γ*(Car—H)). ^{1}H NMR (500 Hz, DMSO-d_6): *δ* 3.72 (*s*, 3H, OCH_3), 5.26 (*s*, 2H, C6H), 6.79 (*s*, 2H, NH_2), 6.91 (*d*, *J* = 9.0 Hz, 2H, C9H and C11H), 7.21 ppm (*d*, *J* = 9.0 Hz, 2H, C8H and C12H). ^{13}C{^{1}H} NMR (125 Hz, DMSO-d_6): *δ* 47.11 (C6), 55.13 (OCH_3), 114.08 (C9 and C11), 127.31 (C7), 129.21 (C8 and C12), 155.00 (C5), 159.01 ppm (C10). UV–Vis (DMSO/H_2O, λ_{max}, nm): 238.0 ($\varepsilon = 3.5{\cdot}10^3$ M^{-1} cm^{-1}), 273.0 ($\varepsilon = 1.4{\cdot}10^3$ M^{-1} cm^{-1}). HRMS (HESI/Orbitrap) *m/z* [M+Na]$^+$ calc for $C_9H_{11}N_5ONa$: 228.08613; found 228.08524.

2.3. Synthesis of silver(I) complexes **1**–**3**

Silver(I) complexes with 1-benzyl-1*H*-tetrazoles, $[Ag(NO_3\text{-}O)(bntz\text{-}N4)_2]_n$ (**1**), $[Ag(NO_3\text{-}O)(bntza\text{-}N4)_2]_n$ (**2**) and $[Ag(NO_3\text{-}O)(mbntza\text{-}N4)_2]_n$ (**3**), were synthesized in accordance to the previously described method for the preparation of the silver(I) complexes with diazanaphthalenes [10]. The purity of the complexes was confirmed by elemental microanalysis and NMR spectroscopy.

The solution of 1.0 mmol of the corresponding 1-benzyl-1*H*-tetrazole (160.2 mg of bntz for **1**, 175.2 mg of bntza for **2** and 205.2 mg of mbntza for **3**) in 5.0 mL of ethanol was added slowly under stirring to the solution containing an equimolar amount of $AgNO_3$ (169.9 mg) in 10.0 mL of ethanol. The reaction mixture was stirred for 3–4 h on a magnetic stirrer, in a sealed round-bottom flask, protected from light at room temperature. Complexes **1** and **3** were obtained from the mother ethanol solution after its cooling in the refrigerator for several days. The crystals of complex **2** were obtained after the crude product, resulting from the reaction of $AgNO_3$ and bntza, was dissolved in 10 mL of acetonitrile. Yield (calculated on the basis of the *N*-heterocyclic ligand): 152.0 mg (62%) for **1**, 189.9 mg (73%) for **2** and 191.5 mg (66%) for **3**.

Anal. Calc. for **1** ($C_{16}H_{16}AgN_9O_3$; MW = 490.25): C, 39.20; H, 3.29; N, 25.71. Found: C, 38.87; H, 3.22; N, 26.04%. IR (KBr, *ν*, cm^{-1}): 3113 (*ν*(C_{ar}—H)), ~3000 (*ν*(C—H)), 1654 (*ν*(C_{ar}=N)), 1494 (*ν*(N—C_{ar}=N)), 1384, 1354 (ν_{as}(NO_3)), 1244 (*ν*(C—N)), 1164 (*ν*(N—N)), 711 (*γ*(Car—H)). ^{1}H NMR (400 Hz, DMSO-d_6): *δ* 5.72 (*s*, 2H, C6H), 7.30–7.44 (*m*, 5H, C8H–C12H), 9.53 ppm (*s*, 1H, C5H). ^{13}C{^{1}H} NMR (101 Hz, DMSO-d_6): *δ* 51.26 (C6), 128.62 (C8 and C12), 128.94 (C10), 129.37 (C9 and C11), 135.31 (C7), 144.51 ppm (C5). UV–Vis (DMSO/H_2O, λ_{max}, nm): 257.0 ($\varepsilon = 5.3{\cdot}10^2$ M^{-1} cm^{-1}).

Anal. Calc. for **2** ($C_{16}H_{18}AgN_{11}O_3$; MW = 520.28): C, 36.94; H, 3.49; N, 29.62. Found: C, 36.65; H, 3.62; N, 29.88%. IR (KBr, *ν*, cm^{-1}): 3322 (ν_{as}(NH_2)), 3203 (ν_s(NH_2)), ~3000 (*ν*(C_{ar}—H) and *ν*(C—H)), 1647 (*ν*(C_{ar}=N)), 1483 (*ν*(N—C_{ar}=N)), 1440 (*δ*(CH_2)), 1384, 1364 (ν_{as}(NO_3)), 1334 (*ν*(N=N)), 1204 (*ν*(C—N)), 1144 (*ν*(N—N)), 708 (*γ*(Car—H)). ^{1}H NMR (400 Hz, DMSO-d_6): *δ* 5.38 (*s*, 2H, C6H), 6.90 (*s*, 2H, NH_2), 7.24 (*d*, *J* = 6.9 Hz, 2H, C8H and C12H), 7.33 (*d*, *J* = 7.1 Hz, 1H, C10H), 7.38 ppm (*t*, *J* = 7.1 Hz, 2H, C9H and C11H). ^{13}C{^{1}H} NMR (101 Hz, DMSO-d_6): *δ* 48.12 (C6), 128.02 (C8 and C12), 128.44 (C10), 129.19 (C9 and C11), 135.79 (C7), 155.96 ppm (C5). UV–Vis (DMSO/H_2O, λ_{max}, nm): 239.0 ($\varepsilon = 2.1{\cdot}10^3$ M^{-1} cm^{-1}).

Anal. Calc. for **3** ($C_{18}H_{22}AgN_{11}O_5$; MW = 580.31): C, 37.25; H, 3.82; N, 26.55. Found: C, 36.60; H, 3.63; N, 26.19%. IR (KBr, *ν*, cm^{-1}): 3337 (ν_{as}(NH_2)), 3160 (ν_s(NH_2)), ~3000 (*ν*(C_{ar}—H) and *ν*(C—H)), 1656 (*ν*(C_{ar}=N)), 1514 (*ν*(N—C_{ar}=N)), 1478 (*δ*(CH_3)), 1441 (*δ*(CH_2)), 1384, 1306 (ν_{as}(NO_3)), 1253 (*ν*(C—O)), 1181 (*ν*(N—N)), 792 (*γ*(Car—H)). ^{1}H NMR (400 Hz, DMSO-d_6): *δ* 3.73 (*s*, 3H, OCH_3), 5.28 (*s*, 2H, C6H), 6.86 (*s*, 2H, NH_2), 6.92 (*d*, *J* = 8.6 Hz, 2H, C9H and C11H), 7.22 ppm (*d*, *J* = 8.6 Hz, 2H, C8H and C12H). ^{13}C{^{1}H} NMR (101 Hz, DMSO-d_6): *δ* 47.64 (C6), 55.60 (OCH_3), 114.56 (C9 and C11), 127.70 (C7), 129.70 (C8 and C12), 155.73 (C5), 159.49 ppm (C10). UV–Vis (DMSO/H_2O, λ_{max}, nm): 238.0 ($\varepsilon = 3.4{\cdot}10^3$ M^{-1} cm^{-1}), 273.0 ($\varepsilon = 1.4{\cdot}10^3$ M^{-1} cm^{-1}).

2.4. Crystallographic data collection and refinement of the structures

Crystal data and details of the structure determinations are compiled in Table 1. Full shells of intensity data were collected

Table 1
Details of the crystal structure determinations of the silver(I) complexes **1** and **2**.

	1	**2**
Empirical formula	$C_{16}H_{16}AgN_9O_3$	$C_{16}H_{18}AgN_{11}O_3$
Formula weight	490.25	520.28
Crystal system, space group	orthorhombic, $Pna2_1$	triclinic, $P\bar{1}$
a (Å)	15.2438(4)	11.8862(3)
b (Å)	22.2842(5)	12.3342(2)
c (Å)	5.49642(15)	15.4198(3)
α (°)		106.1444(16)
β (°)		112.1390(19)
γ (°)		95.7894(18)
V (Å^3)	1867.11(8)	1956.92(7)
F_{000}	984	1048
Z	4	4
X-radiation, λ (Å)	Cu-K$_\alpha$ 1.54184	Mo-K_α 0.71073
Data collect. temperat. (K)	120(1)	120(1)
Calculated density (Mg m^{-3})	1.744	1.766
Absorption coefficient (mm^{-1})	9.023	1.077
Crystal size (mm^3)	0.087 × 0.050 × 0.023	0.099 × 0.089 × 0.057
θ (°)	3.5–71.0	2.3–32.5
Index ranges h, k, l	−18…18, −27…27, −6…6	−17…17, −18…18, −23…23
No. of collected, independent and observed [$I > 2\sigma(I)$] reflections	59328, 3589, 3313	48945, 13254, 8558
R_{int}	0.0471	0.0392
Transmission factors: max, min	0.852, 0.574	1.0000, 0.9795
Data/restraints/parameters	3589/1/262	13 254/0/583
Goodness-on-fit on F^2	1.052	1.016
Final R indices [$F_o > 4\sigma(F_o)$] $R(F)$, $wR(F^2)$	0.0444, 0.1129	0.0338, 0.0676
Final R indices (all data) $R(F)$, $wR(F^2)$	0.0483, 0.1167	0.0642, 0.0787
Absolute structure parameter	0.008(4)	
Difference density: rms, max, min (e Å^{-3})	0.112, 0.460, −1.490	0.092, 0.557, −0.425
CCDC deposition number	1851085	1851086

at low temperature with an Agilent Technologies Supernova-E CCD diffractometer (Mo or Cu Kα radiation, microfocus X-ray tube, multilayer mirror optics). Detector frames (typically ω-, occasionally φ-scans, scan width 0.4…1°) were integrated by profile fitting [47,48]. Data were corrected for air and detector absorption, Lorentz and polarization effects and scaled essentially by application of appropriate spherical harmonic functions [48–50]. Absorption by the crystal was treated with a semiempirical multiscan method (as part of the scaling process) and augmented by a spherical correction [49,50] or numerically (Gaussian grid) [48,51]. An illumination correction was performed as part of the numerical absorption correction [49]. The structures were solved by "modern" direct methods with dual-space recycling (VLD procedure [52], complex **1**) or by intrinsic phasing [53] and refined by full-matrix least squares methods based on F^2 against all unique reflections [54]. All non-hydrogen atoms were given anisotropic displacement parameters. Hydrogen atoms were generally input at calculated positions and refined with a riding model. The positions of the hydrogen atoms of the amino groups in **2** were taken from difference Fourier syntheses and refined. MERCURY computer graphics program was used to prepare drawings [55].

2.5. Quantum-mechanical calculations

All DFT calculations were carried out at the B3LYP level of theory using 6-31G**+ basis set in Jaguar from Schrödinger Suite 2018-1 (Schrödinger Release 2018-1: Jaguar, Schrödinger, LLC, New York, NY, 2018.). The B3LYP method is known to give good descriptions of transition metal complexes [56]. All structures were prepared in Schrödinger Suite and optimized in Jaguar using same aforementioned parameters prior to calculation.

2.6. Antimicrobial studies

MIC concentrations of **1**–**3** and 1-benzyl-1*H*-tetrazole ligands were determined according to the standard broth microdilution assays, recommended by the National Committee for Clinical Laboratory Standards (M07-A8) for bacteria and Standards of European Committee on Antimicrobial Susceptibility Testing (v 7.3.1: Method for the determination of broth dilution minimum inhibitory concentrations of antifungal agents for yeasts) for *Candida* spp. The tested compounds were dissolved in DMSO at 50 mg/mL. The highest concentration used was 500 μg/mL. Bacterial test organisms included: *Staphylococcus aureus* ATCC 25923, *Listeria monocytogenes* NCTC 11994, *Micrococcus luteus* ATCC 379, *Pseudomonas aeruginosa* PAO1 NCTC 10322, and *Candida* strains: *C. albicans* ATCC 10231, *C. glabrata* ATCC 2001, *C. krusei* ATCC 6258, *C. parapsilosis* ATCC 22019. The inoculums were 10^5 colony forming units, cfu/mL, for bacteria and 10^4 cfu/mL for *Candida spp*. The MIC value was recorded as the lowest concentration that inhibited the growth after 24 h at 37 °C.

2.7. In vitro cytotoxicity assay

Cell viability was tested by the 3-(4,5-dimethylthiazol-2-yl)-2,5-diphenyltetrazolium bromide (MTT) assay [57]. The assay was carried out using human lung fibroblasts (MRC5) after 48 h of cell incubation in the media, containing compounds at concentrations ranging from 0.2 to 200 μg/mL. The MRC5 cell line was maintained in the RPMI-1640 medium, supplemented with 100 μg/mL streptomycin, 100 U/mL penicillin and 10% (v/v) fetal bovine serum (FBS) (all from Sigma, Munich, Germany) as a monolayer (1×10^4 cells per well) and grown in humidified atmosphere of 95% air and 5% CO_2 at 37 °C. The extent of MTT reduction was measured spectrophotometrically at 540 nm using a Tecan Infinite 200 Pro multiplate reader (Tecan Group Ltd., Männedorf, Switzerland), and the cell survival was expressed as percentage of the control (untreated cells). The percentage viability values were plotted against the log of concentration and a sigmoidal dose response curve was calculated by non-linear regression analysis, using the Graphpad Prism software, version 5.0 for Windows (Graphpad Software, CA, USA). Cytotoxicity is expressed as the concentration of the compound inhibiting growth by 50% (IC_{50}).

3. Results and discussion

3.1. Synthesis and structural characterization of 1-benzyl-1H-tetrazoles and the silver(I) complexes 1–3

Three tetrazole-containing compounds, 1-benzyl-1*H*-tetrazole (bntz), 1-benzyl-1*H*-tetrazol-5-amine (bntza) and 1-(4-methoxybenzyl)-1*H*-tetrazol-5-amine (mbntza), were synthesized by the previously reported methods (Scheme S1) [45,46]. They further reacted with $AgNO_3$ in 1:1 mole ratio in ethanol at room temperature to yield $[Ag(NO_3\text{-}O)(bntz\text{-}N4)_2]_n$ (**1**), $[Ag(NO_3\text{-}O)(bntza\text{-}N4)_2]_n$ (**2**) and $[Ag(NO_3\text{-}O)(mbntza\text{-}N4)_2]_n$ (**3**) complexes (Scheme 1). In complexes **1**–**3**, the corresponding tetrazole ligand is monodentatedly coordinated to Ag(I) ion *via* the N4 nitrogen atom.

3.1.1. Spectroscopic characterization

The NMR (^{1}H and ^{13}C), IR and UV–Vis spectroscopic data for the 1-benzyl-1*H*-tetrazoles and the corresponding silver(I) complexes **1**–**3** are given in the Experimental section. The ^{1}H and ^{13}C NMR spectra for **1**–**3** are similar to those of the uncoordinated

1-benzyl-1*H*-tetrazoles and, in most cases, only small shifts of the proton and carbon signals for complexes **1**–**3** with respect to those for the ligands are observed, what seems to be a spectroscopic feature of silver(I) complexes in solution [16]. All proton signals of **1**–**3** are shifted downfield in respect to those of the corresponding 1-benzyl-1*H*-tetrazoles. The chemical shifts of the protons after ligand coordination to Ag(I) are strongly dependent on the proton position relative to the metal ion. Of particular note is the shifting of NMR signal of the proton adjacent to the N4 tetrazole nitrogen binding center, *i.e.* C5H proton, in the spectrum of **1**. Thus, C5H in the spectrum of uncoordinated bntz gives a singlet at δ 8.57 ppm, and it was shifted downfield at 9.53 ppm ($\Delta\delta$ = 0.96 ppm) after its coordination to the Ag(I) ion. For the complexes **1**–**3**, ^{1}H NMR spectra remained unmodified over 48 h, indicating their stability in solution during that time. More specifically, no decomposition of the complexes to the free ligands and no coordination of DMSO to Ag(I) were observed.

From the ^{13}C spectra of the complex **1**, it can be concluded that bntz is coordinated to the Ag(I) ion through the N4 tetrazole nitrogen, considering the large shift ($\Delta\delta$ = 2.13 ppm) for the N4 adjacent carbon, C5, compared to the uncoordinated bntz. On the other hand, only a small shift of ~1 ppm is observed for the carbon atoms of bntza and mbntza after their coordination to Ag(I).

The IR spectra of the complexes **1**–**3**, in comparison to those of 1-benzyl-1*H*-tetrazoles, display certain differences which may give an insight in the type of bonds and their structures. A band attributed to the nitrate asymmetric stretching vibrations in the IR spectra of **1**–**3** is split into two bands with relatively small separation, being an indication of nitrate coordination in these complexes [58]. The splitting of the nitrate asymmetric stretching vibrations in the

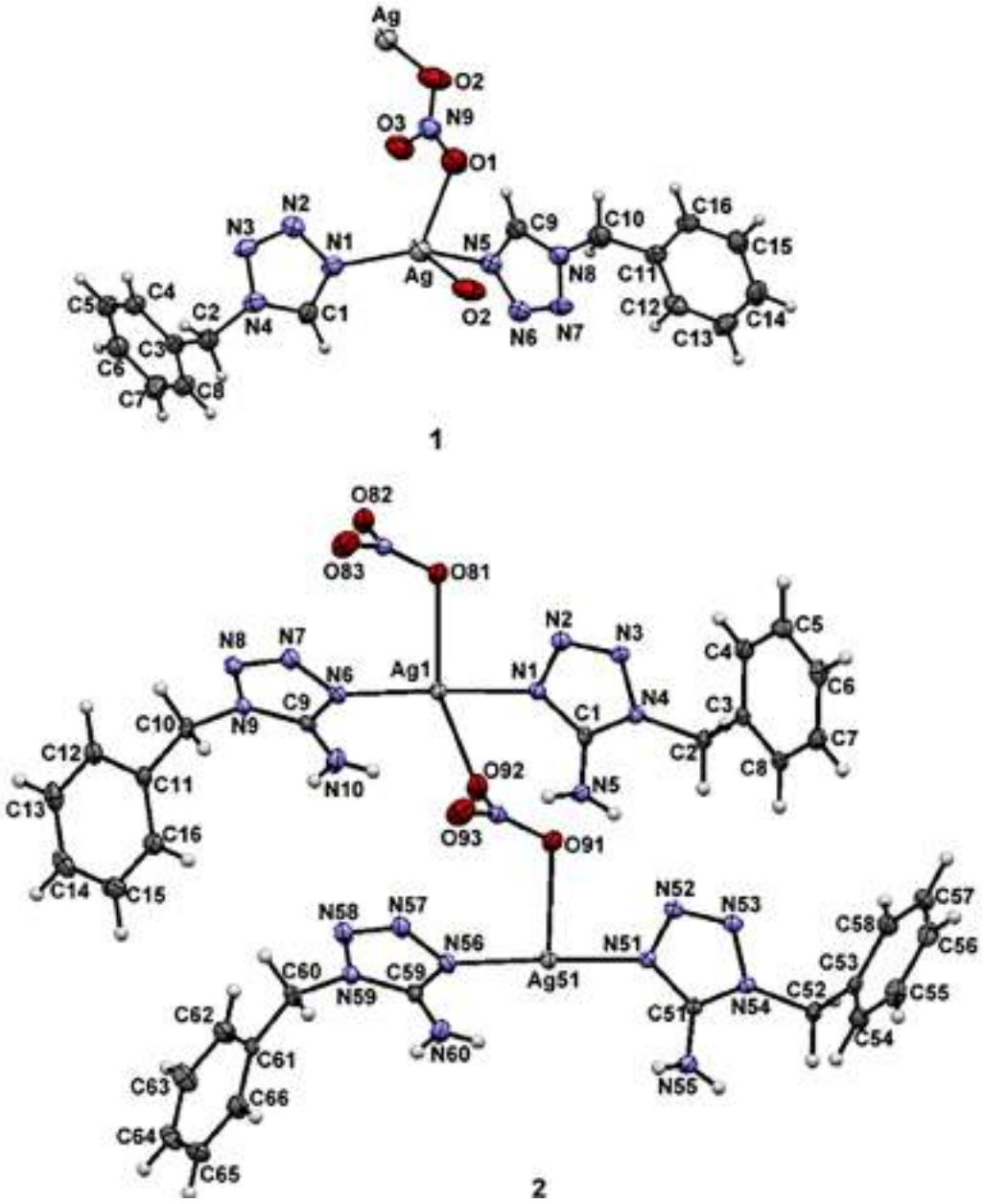

Fig. 1. Molecular structures of silver(I) complexes **1** and **2**. Displacement ellipsoids are drawn at 50% probability level and H atoms are represented by spheres of arbitrary size.

IR spectra of **1**–**3** is in accordance with that observed for the polynuclear $[Ag(NO_3)(qz)]_n$ complex (qz is quinazoline) which contains nitrate as a bridging ligand between two Ag(I) ions [9]. The IR spectra of complexes **2** and **3** also show the expected bands at approximately 3300 and 3200 cm^{-1}, which are due to the asymmetric and symmetric stretching vibrations of the amino group, respectively [59].

The UV–Vis spectra of silver(I) complexes **1**–**3**, recorded in DMSO/H_2O, resemble those of the corresponding 1-benzyl-1*H*-tetrazole ligands. In the complexes **1** and **2**, the corresponding absorbance peaks at ~257.0 and 239.0 nm, respectively, are caused by the characteristic $\pi \rightarrow \pi^*$ transitions in the ligand [60,61]. The absorbance peak for **2** shows slight red shift compared to that for the free ligand (λ = 238.0 nm). The UV–Vis spectra of mbntza and the corresponding complex **3** have two maximum absorbance peaks at 238.0 and 273.0 nm, which can be assigned to $\pi \rightarrow \pi^*$ transition of the phenyl ring and $n \rightarrow \pi^*$ intraligand transition of its methoxy group, respectively [62].

3.1.2. Description of the single crystal structures

The molecular structures of complexes **1** and **2** with the crystallographic numbering scheme are depicted in Fig. 1. The relevant bond distances and angles with their estimated standard deviations are presented in Table 2.

Silver(I) complex **1** with 1-benzyl-1*H*-tetrazole is polynuclear. Each Ag(I) ion is surrounded by two bntz ligands, which are coordinated *via* the nitrogen adjacent to the tetrazole carbon (N1 and N5, Fig. 1) and by two nitrates. Two Ag(I) ions are connected by one nitrate, which behaves as bidentate bridging ligand (d(Ag—O) = 2.506(7) and 2.491(6) Å). The coordination geometry around Ag(I) in distorted tetrahedral, what emerges from the τ_4 parameter of 0.70, $\tau_4 = [360° - (\beta + \alpha)]/141°$, where β and α are the largest angles involving the metal center (square-planar and tetrahedral geometries result in τ_4 values of 0 and 1) [63]. The average Ag—N(tetrazole) and Ag—O(nitrate) bond distances are 2.252 and 2.498 Å, respectively (Table 2) and compare well with those found in the other pseudo tetrahedral silver(I) complexes [64–66].

Similar to **1**, silver(I) complex **2** contains two monodentatedly coordinated 1-benzyl-1*H*-tetrazol-5-amine *via* the nitrogen adjacent to the tetrazole carbon (N1/N51 and N6/N56, Fig. 1). The coordinated tetrazole nitrogens of the two bntza ligands are almost equidistant from the Ag(I) ion (Table 2) and are in agreement with the other silver(I) complexes with aromatic *N*-heterocycles [10]. One of the nitrate oxygens acts as acceptor in bifurcated hydrogen bonding with the amino groups of both tetrazolamino ligands on the same silver(I) ion (Table 3). An additional comparatively weak interaction of two nitrate oxygens with the silver(I) ions leads to polymeric Ag-(NO_3)-Ag-(NO_3)- chains (Table 2). Interestingly, an ordered superstructure with a dinuclear $[Ag(NO_3)(bntza)_2]_2$ repetition unit is formed, with the only significant difference between the two very similar mononuclear subunits being the rotational conformations of the benzyl substituents.

Table 2
Selected bond distances (Å) and valence angles (°) in silver(I) complexes **1** and **2**.

1		**2**	
Ag—O1	2.506(7)	Ag1—N1	2.1155(16)
Ag—O2^{i}	2.491(6)	Ag1—N6	2.1100(17)
Ag—N1	2.241(5)	Ag51—N51	2.1202(17)
Ag—N5	2.264(5)	Ag51—N56	2.1145(17)
O1—N9	1.259(11)	Ag1—O81	2.6859(16)
O2—N9	1.241(11)	Ag1—O92	2.8882(15)
O3—N9	1.255(7)	Ag51—O82^{iii}	2.8644(15)
		Ag51—O91	2.6579(16)
O1—Ag—O2^{i}	83.80(15)	N1—Ag1—N6	175.67(7)
N1—Ag—O1	112.9(2)	N2—N1—Ag1	121.14(3)
N1—Ag—O2^{i}	101.7(2)	C1—N1—Ag1	131.99(14)
N1—Ag—N5	148.56(18)	N7—N6—Ag1	122.22(13)
N5—Ag—O1	95.6(2)	C9—N6—Ag1	130.58(14)
N5—Ag—O2^{i}	93.9(2)	N51—Ag51—N56	174.66(7)
N9—O1—Ag	100.0(5)	N52—N51—Ag51	122.78(13)
N9—O2—Ag^{ii}	103.9(4)	C51—N51—Ag51	130.32(14)
N2—N1—Ag	123.4(4)	N57—N56—Ag51	120.84(13)
C1—N1—Ag	129.8(4)	C59—N56—Ag51	132.34(14)
N6—N5—Ag	122.7(4)		
C9—N5—Ag	130.4(5)		

Symmetry code: (i) $x, y, z-1$; (ii) $x, y, z+1$; (iii) $x, 1+y, z$.

3.2. Computational studies

In order to gain a better understanding of the coordination mode of the synthesized 1-benzyl-1*H*-tetrazoles toward the Ag(I) ion, the structures of bntz and bntza were optimized and their molecular electrostatic potential (MEP) mapped on electron density surface generated at B3LYP/6-31G**+ level of theory was examined (Fig. 2a). The MEP is a useful property for analyzing and predicting the sites or regions of a molecule to which an approaching electrophile (metal ion) is initially attracted [67,68]. The regions of negative potential are colored in red, while the blue regions have positive potential. From Fig. 2a, one could see that in bntz and bntza molecules, the negative electrostatic region is localized on the N3 and N4 tetrazole nitrogens, indicating that both of these donors are almost equally accessible to metal ion. However, the results of calculations suggest that the electron density in the HOMO (Highest Occupied Molecular Orbital) is mainly distributed over the tetrazole ring, and some slight preference for the coordinating nitrogen atom N4 could be found (Fig. 2b). These theoretical findings are in line with the X-ray results for the complexes **1** and **2**, all together supporting the selective formation of silver(I) complexes in which the corresponding tetrazole-containing ligand is coordinated *via* the nitrogen which is adjacent to the tetrazole carbon atom.

3.3. Antimicrobial and cytotoxic activity of the 1-benzyl-1H-tetrazoles and silver(I) complexes ***1***–***3***

Given the traditional antimicrobial effects exerted by silver-containing materials and compounds, the antimicrobial effects of the newly synthesized complexes **1**–**3**, as well as the corresponding ligands have been evaluated against the panel of bacteria and

Table 3
Hydrogen bond parameters for silver(I) complex **2**.

D—H···*A*	*D*—H (Å)	H···*A* (Å)	*D*···*A* (Å)	*D*—H···*A* (°)
N5—H5a···O92	0.88(2)	1.97(2)	2.839(2)	170(2)
N10—H10B···O83^{i}	0.82(3)	2.06(3)	2.866(3)	169(3)
N55—H55A···O82^{ii}	0.81(2)	2.04(3)	2.847(2)	171(2)
N60—H60B···O93^{iii}	0.80(3)	2.08(3)	2.862(3)	164(3)

Symmetry codes: (i) $-x+2, -y+1, -z+2$; (ii) $x, y+1, z$; (iii) $-x+2, -y+2, -z+2$.

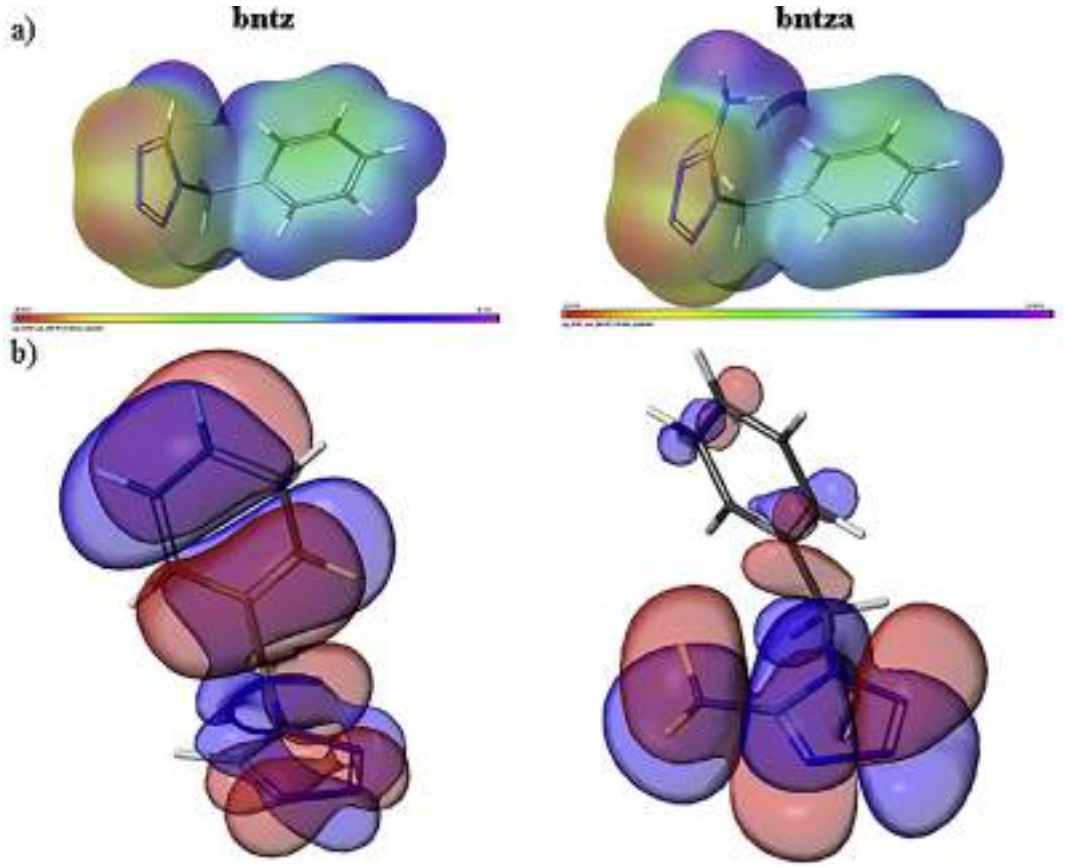

Fig. 2. (a) Electrostatic potential mapped on electron density surfaces for the bntz and bntza generated at DFT B3LYP/6-31G**+ level of theory (isoval 0.0025 a.u.). Color change from red most negative to blue most positive. (b) HOMO orbitals of bntz and bntza. (Color online.)

Table 4
Minimal inhibitory concentrations (MIC) against a panel of microorganisms and antiproliferative activity (IC_{50}) of **1**–**3**.

	Compound					
	1		**2**		**3**	
Organism	μg/mL	μM	μg/mL	μM	μg/mL	μM
Staphylococcus aureus	4	8.2	2	3.8	4	6.9
Listeria monocytogenes	4	8.2	2	3.8	8	13.8
Micrococcus luteus	8	16.3	2	3.8	4	6.9
Pseudomonas aeruginosa PAO1	2	4.1	2	3.8	4	6.9
Candida albicans	0.62	1.26	0.62	1.19	1.25	2.15
Candida glabrata	0.62	1.26	0.62	1.19	1.25	2.15
Candida krusei	0.62	1.26	0.31	0.60	0.62	1.07
Candida parapsilosis	0.16	0.33	0.16	0.31	0.31	0.53
MRC5 (human lung fibroblasts)[a]	50	102.0	30	57.7	60	103.4

[a] IC_{50} is defined as the concentration inhibiting 50% of cell growth after 48 h treatment with the tested compounds. Results are from three independent experiments, each performed in triplicate. Standard deviations were within 1–3%.

Candida strains (Table 4). While 1-benzyl-1*H*-tetrazoles used for the synthesis of the silver(I) complexes were not active against the investigated strains at concentrations higher than 500 μg/mL (data not shown), **1**–**3** showed growth inhibiting activity against all tested strains, suggesting that the activity of the complexes originates from the presence of Ag(I) ions. The MIC values of the silver(I) complexes were between 2 and 8 μg/mL (3.8–16.3 μM) against bacterial strains, while they were able to inhibit *Candida*, both *albicans* and non-*albicans* strains at 0.16–1.25 μg/mL (0.31–2.15 μM) MIC concentration values (Table 4). Three complexes exhibited comparable activity, with **2** being slightly more active across the microbial panel. From these data, no difference has been observed between Gram-positive and Gram-negative strains, while anti-*Candida* activity of these complexes was more prominent, with *C. parapsilosis* being the most sensitive strain. More importantly, **1**–**3** were moderately cytotoxic against human lung fibroblast cell line, with the best selectivity index being 312 (for **1** and *C. parapsilosis*) giving reason for further evaluations of these complexes for therapeutic applications. These results are of special importance having in mind, that emerging non-*albicans Candida* species, such as *C. parapsilosis*, *C. glabrata*, *C. tropicalis* and *C. krusei*, are increasingly recognized as causative agents of infections ranging from superficial to life-threatening disseminated bloodstream and deep-tissue infections [69].

Good antimicrobial activity of **1**–**3** was comparable or slightly better to that observed for silver(I) complexes with aromatic nitrogen-containing heterocycles such as pyridazine, pyrimidine, pyrazine, quinoxaline, phenazine, quinazoline and phthalazine

[9,10,26]. Unlike these complexes, **1**–**3** showed higher activity against selection of *Candida* strains. Improved activity against *C. albicans* in comparison to the antibacterial activity has also been observed for silver(I) complexes with coordinated 4-(hydroxymethyl)pyridine, 2,6-di(hydroxymethyl)pyridine and 2-(hydroxymethyl)benzimidazole (MIC = 10–20 μg/mL) [23]. Notably, **1**–**3** did not cause significant cytotoxic effect *in vitro*, which is usually observed with Ag(I) complexes [9].

4. Conclusions

We have demonstrated that the tetrazole-containing ligands, 1-benzyl-1*H*-tetrazole (bntz), 1-benzyl-1*H*-tetrazol-5-amine (bntza) and 1-(4-methoxybenzyl)-1*H*-tetrazol-5-amine (mbntza), can selectively bind to the Ag(I) ion *via* the nitrogen atom N4 which is adjacent to the carbon atom of the tetrazole ring. All these ligands coordinate to the Ag(I) ion to form polynuclear species, in which nitrate acts as a bridging ligand between two Ag(I) ions. Of a series of the investigated silver(I) complexes, the best antimicrobial activity against the investigated fungal and bacterial strains is observed for the silver(I) complex $[Ag(NO_3\text{-}O)(bntza\text{-}N4)_2]_n$, with tetrazole ligand containing the amino group and unsubstituted benzyl ring. At the same time, this complex is the most cytotoxic; nevertheless, its selectivity indices are, in some cases, higher than 180. These findings serve as a basis for further design of tetrazole-containing compounds, which could be used as ligands for complexation of Ag(I) ion, what can be of importance for the development of novel silver-based antimicrobials.

Acknowledgements

This research has been financially supported by the Ministry of Education, Science and Technological Development of the Republic of Serbia, under Grants No. 172008, 172036 and 173048, the SupraMedChem@Balkans.Net SCOPES Institutional Partnership (Project No. IZ74Z0_160515) and the Serbian Academy of Sciences and Arts (Project No. F128). The authors acknowledge the support of the FP7 RegPot project FCUB ERA GA No. 256716. The EC does not share responsibility for the content of the article.

Appendix A. Supplementary data

CCDC 1851085 and 1851086 contains the supplementary crystallographic data for this paper. These data can be obtained free of charge via http://www.ccdc.cam.ac.uk/conts/retrieving.html, or from the Cambridge Crystallographic Data Centre, 12 Union Road, Cambridge CB2 1EZ, UK; fax: (+44) 1223-336-033; or e-mail: deposit@ccdc.cam.ac.uk. Supplementary data associated with this article can be found, in the online version, at https://doi.org/10.1016/j.poly.2018.08.001.

References

[1] F. Marchetti, J. Palmucci, C. Pettinari, R. Pettinari, S. Scuri, I. Grappasonni, M. Cocchioni, M. Amati, F. Lelj, A. Crispini, Inorg. Chem. 55 (2016) 5453–5466.
[2] A.N. Khlobystov, A.J. Blake, N.R. Champness, D.A. Lemenovskii, A.G. Majouga, N. V. Zyk, M. Schröder, Coord. Chem. Rev. 222 (2001) 155–192.
[3] K.M. Fromm, Nat. Chem. 3 (2011) 178.
[4] K.M. Fromm, Appl. Organomet. Chem. 27 (2013) 683–687.
[5] S. Eckhardt, P.S. Brunetto, J. Gagnon, M. Priebe, B. Giese, K.M. Fromm, Chem. Rev. 113 (2013) 4708–4754.
[6] S. Medici, M. Peana, G. Crisponi, V.M. Nurchi, J.I. Lachowicz, M. Remelli, M.A. Zoroddu, Coord. Chem. Rev. 327–328 (2016) 349–359.
[7] P. Kleyi, R.S. Walmsley, M.A. Fernandes, N. Torto, Z.R. Tshentu, Polyhedron 41 (2012) 25–29.
[8] A.B.G. Lansdown, Crit. Rev. Toxicol. 37 (2007) 237–250.
[9] N.D. Savić, B.Đ. Glišić, H. Wadepohl, A. Pavic, L. Senerovic, J. Nikodinovic-Runic, M.I. Djuran, MedChemComm 7 (2016) 282–291.
[10] B.Đ. Glišić, L. Senerovic, P. Comba, H. Wadepohl, A. Veselinovic, D.R. Milivojevic, M.I. Djuran, J. Nikodinovic-Runic, J. Inorg. Biochem. 155 (2016) 115–128.
[11] I. Tsyba, B. Bun-kit Mui, R. Bau, R. Noguchi, K. Nomiya, Inorg. Chem. 42 (2003) 8028–8032.
[12] K. Nomiya, S. Takahashi, R. Noguchi, S. Nemoto, T. Takayama, M. Oda, Inorg. Chem. 39 (2000) 3301–3311.
[13] K. Nomiya, K. Tsuda, T. Sudoh, M. Oda, J. Inorg. Biochem. 68 (1997) 39–44.
[14] J.A. Joule, M. Keith, Heterocyclic Chemistry, Blackwell Science, Oxford, 2000.
[15] M. McCann, R. Curran, M. Ben-Shoshan, V. McKee, M. Devereux, K. Kavanagh, A. Kellett, Polyhedron 56 (2013) 180–188.
[16] U. Kalinowska-Lis, A. Felczak, L. Chęcińska, K. Zawadzka, E. Patyna, K. Lisowska, J. Ochocki, Dalton Trans. 44 (2015) 8178–8189.
[17] U. Kalinowska-Lis, A. Felczak, L. Chęcińska, M. Małecka, K. Lisowska, J. Ochocki, New J. Chem. 40 (2016) 694–704.
[18] R. Rowan, T. Tallon, A.M. Sheahan, R. Curran, M. McCann, K. Kavanagh, M. Devereux, V. McKee, Polyhedron 25 (2006) 1771–1778.
[19] K. Nomiya, R. Noguchi, M. Oda, Inorg. Chim. Acta 298 (2000) 24–32.
[20] S.H. Alisir, B. Sariboga, Y. Topcu, S.-Y. Yang, J. Inorg. Organomet. Polym. 23 (2013) 1061–1067.
[21] Z. Vargová, M. Almáši, D. Hudecová, D. Titková, I. Rostášová, V. Zeleňák, K. Györyová, J. Coord. Chem. 67 (2014) 1002–1021.
[22] S.H. Alisir, S. Demir, B. Sariboga, O. Buyukgungor, J. Coord. Chem. 68 (2015) 155–168.
[23] U. Kalinowska-Lis, A. Felczak, L. Chęcińska, K. Lisowska, J. Ochocki, J. Organomet. Chem. 749 (2014) 394–399.
[24] U. Kalinowska-Lis, A. Felczak, L. Chęcińska, I. Szabłowska-Gadomska, E. Patyna, M. Małecki, K. Lisowska, J. Ochocki, Molecules 21 (2016) 87–100.
[25] A.A.A. Massoud, V. Langer, Y.M. Gohar, M.A.M. Abu-Youssef, J. Jänis, G. Lindberg, K. Hansson, L. Öhrström, Inorg. Chem. 52 (2013) 4046–4060.
[26] N.D. Savić, D.R. Milivojevic, B.Đ. Glišić, T. Ilic-Tomic, J. Veselinovic, A. Pavic, B. Vasiljevic, J. Nikodinovic-Runic, M.I. Djuran, RSC Adv. 6 (2016) 13193–13206.
[27] S. Aslam, A.A. Isab, M.A. Alotaibi, M. Saleem, M. Monim-ul-Mehboob, S. Ahmad, I. Georgieva, N. Trendafilova, Polyhedron 115 (2016) 212–218.
[28] M.A. Fik, A. Gorczynski, M. Kubicki, Z. Hnatejko, A. Fedoruk-Wyszomirska, E. Wyszko, M. Giel-Pietraszuk, V. Patroniak, Eur. J. Med. Chem. 86 (2014) 456–468.
[29] M. McCann, M. Geraghty, M. Devereux, D. O'Shea, J. Mason, L. O'Sullivan, Met. Based Drugs 7 (2000) 185–193.
[30] B. Coyle, K. Kavanagh, M. McCann, M. Devereux, M. Geraghty, BioMetals 16 (2003) 321–329.
[31] B. Coyle, P. Kinsella, M. McCann, M. Devereux, R. O'Connor, K. Kavanagh, Toxicol. In Vitro 18 (2004) 63–70.
[32] M. McCann, B. Coyle, S. McKay, P. McCormack, K. Kavanagh, M. Devereux, V. McKee, P. Kinsella, R. O'Connor, M. Clynes, BioMetals 17 (2004) 635–645.
[33] A. Eshwika, B. Coyle, M. Devereux, M. McCann, K. Kavanagh, BioMetals 17 (2004) 415–422.
[34] C. Deegan, B. Coyle, M. McCann, M. Devereux, D.A. Egan, Chem.-Biol. Interact. 164 (2006) 115–125.
[35] L. Thornton, V. Dixit, L.O.N. Assad, T.P. Ribeiro, D.D. Queiroz, A. Kellett, A. Casey, J. Colleran, M.D. Pereira, G. Rochford, M. McCann, D. O'Shea, R. Dempsey, S. McClean, A.F.-A. Kia, M. Walsh, B. Creaven, O. Howe, M. Devereux, J. Inorg. Biochem. 159 (2016) 120–132.
[36] N.D. Savić, S. Vojnovic, B.Đ. Glišić, A. Crochet, A. Pavic, G.V. Janjić, M. Pekmezović, I.M. Opsenica, K.M. Fromm, J. Nikodinovic-Runic, M.I. Djuran, Eur. J. Med. Chem. 156 (2018) 760–773.
[37] V.A. Ostrovskii, E.A. Popova, R.E. Trifonov, Adv. Heterocycl. Chem. 123 (2017) 1–62.
[38] C.-X. Wei, M. Bian, G.-H. Gong, Molecules 20 (2015) 5528–5553.
[39] S.V. Voitekhovich, V. Lesnyak, N. Gaponik, A. Eychmüller, Small 11 (2015) 5728–5739.
[40] V.A. Ostrovskii, G.I. Koldobskii, R.E. Trifonov, Comprehensive Heterocyclic Chemistry III: Tetrazoles, Elsevier Ltd., 2008.
[41] G. Aromí, L.A. Barrios, O. Roubeau, P. Gamez, Coord. Chem. Rev. 255 (2011) 485–546.
[42] M.A. Malik, M.Y. Wani, S.A. Al-Thabaiti, R.A. Shiekh, J. Incl. Phenom. Macrocycl. Chem. 78 (2014) 15–37.
[43] D.J.St. Jean Jr., C. Fotsch, J. Med. Chem. 55 (2012) 6002–6020.
[44] A. Mahmooda, I.U. Khan, R.L. Longo, A. Irfan, S.A. Shahzad, C. R. Chim. 18 (2015) 422–429.
[45] Y.H. Joo, J.M. Shreeve, Org. Lett. 10 (2008) 4665–4667.
[46] Y. Satoh, N. Marcopulos, Tetrahedron Lett. 36 (1995) 1759–1762.
[47] K. Kabsch, International Tables for Crystallography Vol. F, Ch. 11.3, Kluwer Academic Publishers, Dordrecht, 2001.
[48] CrysAlisPro, Agilent Technologies UK Ltd., Oxford, UK, 2011-2014, and Rigaku Oxford Diffraction, Rigaku Polska Sp.z o.o., Wrocław, Poland, 2015-2018.
[49] SCALE3 ABSPACK, CrysAlisPro, Agilent Technologies UK Ltd., Oxford, UK, 2011-2014, and Rigaku Oxford Diffraction, Rigaku Polska Sp.z o.o., Wrocław, Poland, 2015-2018.
[50] R.H. Blessing, Acta Crystallogr. Sect. A: Found. Crystallogr. 51 (1995) 33–38.
[51] W.R. Busing, H.A. Levy, Acta Cryst. 10 (1957) 180–182.
[52] (a) M.C. Burla, R. Caliandro, B. Carrozzini, G.L. Cascarano, C. Cuocci, C. Giacovazzo, M. Mallamo, A. Mazzone, G. Polidori, SIR2014, CNR IC, Bari, Italy, 2014;
(b) M.C. Burla, R. Caliandro, B. Carrozzini, G.L. Cascarano, C. Cuocci, C.

Giacovazzo, M. Mallamo, A. Mazzone, G. Polidori, J. Appl. Crystallogr. 48 (2015) 306–309.
[53] (a) G.M. Sheldrick, SHELXT, University of Göttingen and Bruker AXS GmbH, Karlsruhe, Germany, 2012-2018.;
(b) M. Ruf, B.C. Noll, Application Note SC-XRD 503, Bruker AXS GmbH, Karlsruhe, Germany, 2014;
(c) G.M. Sheldrick, Acta Crystallogr. Sect. A: Found. Crystallogr. 71 (2015) 3–8.
[54] (a) G.M. Sheldrick, SHELXL–20xx, University of Göttingen and Bruker AXS GmbH, Karlsruhe, Germany, 2012-2018;
(b) G.M. Sheldrick, Acta Crystallogr. Sect. A: Found. Crystallogr. 64 (2008) 112–122;
(c) G.M. Sheldrick, Acta Crystallogr Sect. C: Cryst. Struct. Commun. 71 (2015) 3–8.
[55] I.J. Bruno, J.C. Cole, P.R. Edgington, M. Kessler, C.F. Macrae, P. McCabe, J. Pearson, R. Taylor, Acta Crystallogr. Sect. B: Struct. Sci. 58 (2002) 389–397.
[56] S. Niu, M.B. Hall, Chem. Rev. 100 (2000) 353–406.
[57] M.B. Hansen, S.E. Nielsen, K. Berg, J. Immunol. Methods 119 (1989) 203–210.
[58] A.S. Potapov, E.A. Nudnova, A.I. Khlebnikov, V.D. Ogorodnikov, T.V. Petrenko, Inorg. Chem. Commun. 53 (2015) 72–75.
[59] S. Chattopadhyay, P. Chakraborty, M.G.B. Drew, A. Ghosh, Inorg. Chim. Acta 362 (2009) 502–508.
[60] J.-A. Zhang, M. Pan, J.-Y. Zhang, H.-K. Zhang, Z.-J. Fan, B.-S. Kang, C.-Y. Su, Polyhedron 28 (2009) 145–149.
[61] Y. Jiang, C.-F. Zhu, Z. Zheng, J.-B. He, Y. Wang, Inorg. Chim. Acta 451 (2016) 143–147.
[62] S.M. Tailor, U.H. Patel, J. Coord. Chem. 68 (2015) 2192–2207.
[63] L. Yang, D.R. Powell, R.P. Houser, Dalton Trans. (2007) 955–964.
[64] C. Pettinari, F. Marchetti, G. Lupidi, L. Quassinti, M. Bramucci, D. Petrelli, L.A. Vitali, M.F.C.G. da Silva, L.M.D.R.S. Martins, P. Smoleński, A.J. Pombeiro, Inorg. Chem. 50 (2011) 11173–11183.
[65] D.L. Reger, E.A. Foley, M.D. Smith, Inorg. Chem. 49 (2010) 234–242.
[66] D.L. Reger, R.P. Watson, J.R. Gardinier, M.D. Smith, Inorg. Chem. 43 (2004) 6609–6619.
[67] F.J. Luque, J.M. López, M. Orozco, Theor. Chem. Acc. 103 (2000) 343–345.
[68] R.V. Pinjari, S.P. Gejji, J. Phys. Chem. A 112 (2008) 12679–12686.
[69] S.G. Whaley, E.L. Berkow, J.M. Rybak, A.T. Nishimoto, K.S. Barker, P.D. Rogers, Front. Microbiol. 7 (2017) 2173.